Understanding the two-dimensional ionization structure in luminous infrared galaxies.
A near-IR integral field spectroscopy perspective

Contents

Abstract

Two-dimensional excitation structure of the ISM with LIRGs and Seyferts using NIR-IFS

[FeII]1.64µm/Brγ – H$_2$2.12µm/Brγ plane → AGNs, young main-sequence stars, evolved stars

- ISM in LIRGs occupy a wide region
    - -0.6 < log([FeII]/Brγ) < 1.5 (median=0.18)
    - -1.2 < log(H$_2$/Brγ) < 0.8 (median=0.04)
- Seyferts: larger value by a factor of ~2.5 ([FeII]/Brγ) and ~1.4 (H$_2$/Brγ)

In addition to the new area and relation for the compact and bright regions,
that for diffuse regions

- AGN diffuse regions: similar area to that of Seyferts but with high [FeII]/Brγ

- Non-AGN diffuse regions: wide area overlapping many mechanism → mixture

Integrated line ratios in LIRGs show higher excitation condition than spatially resolved result

→ Clear consequences when classifying high-z SFG based on NIR integrated spectra

1. Introduction

Characterization of the excitation and ionization conditions

→ the use of strong emission lines for the detection and quantification of them

- Optical emission lines: BPT diagram
- Mid-IR lines: Based on high excitation lines ([NeV]14.32um, [OIV]25.89um) and PAH
(Genzel+1998, ..., Alonso-Herrero+2012)

Near-IR emission line diagnostics

1. Larkin+1998: [FeII]1.26um/Brγ vs $H_2$2.12um/Brγ
Strong linear relation in the log-log plane (low: SFGs→Seyferts→LINERs :high)
2. Rodriguez-Ardila+2004,2005, Riffel+2006: Confirmed the trend reported by Larkin
3. Riffel+2013a: $\log([\text{FeII}]1.26\mu m/\text{Pa}\beta) = 0.749 \times \log(H_2 2.12\mu m/\text{Br}\gamma) - 0.207$
Analysis of Seyfert1, Seyfert2, Star-forming, and a few LINERs

Ionization of the ISM in U/LIRGs in optical: SF, LINER(30-40%), AGN → Complex

The nature of LINER

- galaxy-wide merger-driven shocks
- mixture of starbursts and AGN

← Additional complication by the amount and distribution of dust and tidal forces

→ NIR spatially resolved spectroscopy → More dust-enshrouded SF region and/or obscured AGN

2. Sample of galaxies and observations

2.1. Luminous Infrared galaxies

- Only two galaxies are identified as hosting an AGN

- SINFONI observation

  - Seeing limited H & K

  - $H_2$2.12um, Brγ, [FeII]1.64um maps

  - 1-1.5 kpc radius around nucleus

  - Physical resolution ~ 200pc (FWHM~0.6 arcsec)

- Dust attenuation correction for each region with Brγ/Brδ and Calzetti+2000 (S/N(Brδ)>4) For spaxels where the correction is not available, use median value of the galaxy

- Integrated measurement of the line ratio on different region (emission peaks, K-band peak)

  - Define a circular aperture of 200pc radius, centered on the peak

  - De-rotate each spectra within the aperture and stack (Increase S/N)

  - Fit emission lines using a Gaussian profile

- Uncertainties with a bootstrap method

Table 1

ID1 Common (1)	ID2 IRAS (2)	z (3)	D_L (Mpc) (4)	Scale (pc/") (5)	log $(L_{IR}/L_\odot)$ (6)
NGC 2369	IRAS 07160-6215	0.010807	48.6	230	11.17
NGC 3110	IRAS 10015-0614	0.016858	78.4	367	11.34
NGC 3256	IRAS 10257-4338	0.009354	44.6	212	11.74
ESO 320-G030	IRAS 11506-3851	0.010781	51.1	242	11.35
IRASF 12115-4656	IRAS 12115-4657	0.018489	84.4	394	11.10
NGC 5135	IRAS 13229-2934	0.013693	63.5	299	11.33
IRASF 17138-1017	IRAS 17138-1017	0.017335	75.3	353	11.42
IC 4687	IRAS 18093-5744	0.017345	75.1	352	11.44
NGC 7130	IRAS 21453-3511	0.016151	66.3	312	11.34
IC 5179	IRAS 22132-3705	0.011415	45.6	216	11.12

2. Sample of galaxies and observations

2.2. Nearby Seyfert galaxies

- NIFS/Gemini
- Three Seyfert2, One Seyfert1.5, One Seryfert1
- Cover 300-700 pc around AGN
- Angular resolution ~ 10-100 pc
- Mrk1066 has circumnuclear SF knots within the central 400 pc
- Conversion of [FeII]1.26um/Paβ to [FeII]1.64um/Brγ

$$[FeII]1.64\mu m/Br\gamma = 4.4974 \times [FeII]1.26\mu m/Pa\beta$$ (Case B, T=10,000K, $n_e=10^4 cm^{-3}$)

Table 2

	ID1 Common (1)	ID2 IRAS (2)	z (3)	D_L (Mpc) (4)	Scale (pc/") (5)
Seyfert	Mrk 1157	IRAS 01306+3524	0.015167	61.8	291
	Mrk 1066	IRAS 02568+3637	0.012025	49.2	233
	ESO 428-G014	IRAS 07145-2914	0.005664	27.1	130
	Mrk 79	IRAS 07388+4955	0.022189	98.3	456
	NGC 4151	IRAS Z12080+3940	0.003319	17.8	86
SFG	NGC 693	IRAS 01479+0553	0.005227	18.3	88
	UGC 2855	IRAS 03431+6958	0.004003	15.9	77
	NGC 1569W	IRAS 04260+6444	-0.000347	1.45	7
	M82	IRAS 09517+6954	0.000677	4.03	19
	NGC 4303	IRAS 12194+0444	0.005224	27.5	131
	Mrk 59	IRAS 12566+3507	0.002616	14.7	71
	NGC 7771	IRAS 23488+1949	0.014267	56.6	267

2.3. Nearby star-forming galaxies

- Published line fluxes obtained by Near-IR IFS
- M82: Nucleus, two off-nucleus regions (35x35 pc) and central region (260x160 pc)
- Mrk59: Blue compact dwarf
- NGC4303: Nucleus is classified as LINER – low-luminosity Seyfert2
  Massive($10^5 M_\odot$), UV-luminous, 4 Myr old star cluster
  & a hard X-ray emitting low-luminosity AGN

3. Results

A few to several thousands of spaxels per galaxy → Over 28000 spaxels for all LIRGs

64% of spaxels with a good determination of the A_V

3.1. The characterization of the ISM in LIRGs according to [FeII]1.64μm/Brγ ratio

[FeII]1.64μm/Brγ ~ 0.9 (observed median), 1.5 (dust extinction corrected median)

- No dependence with galaxy, showing a narrow range of values within factors less than 2

- Four galaxies has specific region [FeII]1.64μm/Brγ > 5
  (Nuclei of NGC7130, NGC3110, luminous circumnuclear [FeII] clump of NGC5135
   overall circumnuclear emission in the edge-on galaxy NGC2369)

- Starburst model (number of ionizing photon and related SNe): 0.1 < [FeII]1.64μm/Brγ < 1.4
  and ratio ~1 is reproduced by unlikely IMF (steep and low upper-mass limit~25-30M$_\odot$)
  → SNe-induced shock, X-ray emission in aging starburst, radiation & shocks from an AGN

Table 3: [FeII]1.64μm/Brγ line ratio for all LIRGS. Statistical results from SINFONI/IFS measurements[1]

Object	Median Obs	Median Corr	Mode Obs	Mode Corr	Mean Obs	Mean Corr	σ Obs	σ Corr	P_5 Obs	P_5 Corr	P_{95} Obs	P_{95} Corr	N_{spaxel}
NGC2369	0.61	3.58	0.80	4.02	0.63	3.99	0.23	2.36	0.31	1.40	1.04	7.92	1583
NGC3110	0.72	1.59	0.69	1.73	0.77	1.66	0.23	0.51	0.49	0.96	1.18	2.60	2719
NGC3256	1.06	1.69	0.96	1.82	1.13	2.05	0.39	1.46	0.61	0.79	1.85	4.64	5553
ESO320-G030	0.89	1.37	0.91	1.32	0.91	1.46	0.22	0.52	0.57	0.84	1.30	2.32	4011
IRASF12115-4656	⋯	⋯	⋯	⋯	⋯	⋯	⋯	⋯	⋯	⋯	⋯	⋯	⋯
NGC5135 (all)	0.95	1.89	1.07	1.44	1.21	2.59	0.99	2.25	0.49	1.02	3.24	7.43	1610
NGC5135 ([SiVI])[2]	1.06	2.29	1.07	1.96	1.40	3.03	1.13	2.40	0.48	1.06	4.09	8.32	898
NGC5135 (no [SiVI])[3]	0.80	1.53	0.67	1.37	0.98	2.03	0.71	1.92	0.50	0.97	2.32	4.93	712
IRASF17138-1017	1.05	2.00	1.14	2.08	1.07	2.08	0.36	0.90	0.53	0.83	1.68	3.81	2327
IC4687	0.95	1.60	1.05	1.76	0.97	1.82	0.36	1.01	0.49	0.69	1.55	3.87	4212
NGC7130 (all)	1.18	1.96	0.93	2.01	1.42	3.27	0.85	4.12	0.50	0.75	3.17	10.36	1857
NGC7130 ([SiVI])[2]	2.08	4.60	2.03	4.60	2.20	6.83	0.87	6.29	0.89	1.82	3.86	21.49	498
NGC7130 (no [SiVI])[3]	0.96	1.51	0.94	1.24	1.13	1.96	0.63	1.53	0.49	0.71	2.44	4.77	1359
IC5179	0.55	0.82	0.54	0.85	0.58	0.94	0.18	0.63	0.36	0.42	0.92	1.72	4490
LIRGs	0.87	1.53	0.95	1.46	0.94	1.94	0.49	1.75	0.43	0.62	1.72	4.53	28362

Table 7: [FeII]1.64μm/Brγ line ratios for LIRGs. Values for emission line peaks and integrated measurements

Object	Integrated Obs	Integrated Corr	Nucleus Obs	Nucleus Corr	HII peak Obs	HII peak Corr	H_2 peak Obs	H_2 peak Corr	[FeII] peak Obs	[FeII] peak Corr
NGC2369[1,2]	1.26 ± 0.22	5.33 ± 5.27	0.81 ± 0.06	2.49 ± 0.98	0.83 ± 0.06	2.42 ± 0.89	0.84 ± 0.06	2.49 ± 0.93	1.16 ± 0.10	4.72 ± 2.35
NGC3110[2,3]	0.76 ± 0.09	3.44 ± 1.38	0.76 ± 0.09	5.90 ± 5.97	0.56 ± 0.05	0.99 ± 0.31	0.76 ± 0.09	6.14 ± 6.21	0.75 ± 0.09	4.76 ± 13.03
NGC3256	⋯	⋯	⋯	⋯	⋯	⋯	⋯	⋯	⋯	⋯
ESO320-G030	0.95 ± 0.11	2.36 ± 1.11	1.34 ± 0.60	3.32 ± 2.12	0.74 ± 0.06	1.57 ± 0.53	1.31 ± 0.68	1.96 ± 2.20	1.30 ± 0.54	3.21 ± 1.98
IRASF12115-4656[1,2]	⋯	⋯	⋯	⋯	⋯	⋯	⋯	⋯	⋯	⋯
NGC5135[2]	1.10 ± 0.10	2.79 ± 1.27	1.03 ± 0.06	1.86 ± 0.67	0.74 ± 0.03	1.43 ± 0.34	1.03 ± 0.06	1.86 ± 0.67	3.74 ± 0.15	7.71 ± 3.09
IRASF17138-1017[2]	0.92 ± 0.04	1.58 ± 0.42	1.03 ± 0.03	1.92 ± 0.85	0.55 ± 0.01	0.69 ± 0.11	1.03 ± 0.03	1.92 ± 0.85	0.61 ± 0.01	0.98 ± 0.16
IC4687[4]	0.85 ± 0.04	1.23 ± 0.18	0.93 ± 0.06	2.07 ± 0.63	0.43 ± 0.02	0.61 ± 0.07	1.05 ± 0.08	2.08 ± 0.72	0.47 ± 0.02	0.66 ± 0.08
NGC7130[1,2,3]	1.31 ± 0.09	3.77 ± 3.65	2.44 ± 0.11	5.14 ± 3.90	2.40 ± 0.11	5.11 ± 3.87	2.48 ± 0.11	5.20 ± 4.01	2.44 ± 0.11	5.14 ± 3.90
IC5179[1,2,3]	0.62 ± 0.06	0.97 ± 0.38	0.70 ± 0.05	1.20 ± 0.23	0.68 ± 0.05	1.10 ± 0.21	0.70 ± 0.05	1.14 ± 0.22	0.68 ± 0.05	1.08 ± 0.20

3. Results

3.2 The characterization of the ISM in LIRGs according to H_2/Brγ ratio

H_2/Brγ ~ 0.8 (factor ~1.8-2 lower than that of Seyferts)

- LIRG has lower limit ~ 0.3 like Seyferts(0.4) but upper limit ~2.4 lower than Seyferts(4.0)
  → Excitation mechanism transitions from LIRGs to Seyfert (SF → AGN)

- H_2/Brγ of [SiVI] emitting region in the two LIRGs (NGC5135, NGC7130) ~ Seyferts

Detailed studies of near-IR H_2 line ratio in Seyferts and nearby spirals

- Hot molecular gas is close to thermally excited
  because of a combination of X-ray radiation and shocks

- Brγ is direct tracer of the UV-ionizing radiation

→ H_2/Brγ: Empirical first indication of the relative importance of each mechanism

Table 4: H_2 2.12μm/Brγ line ratio for all LIRGS. Statistical results from SINFONI/IFS measurements[1]

Object	Median		Mode		Mean		σ		P_5		P_{95}		N_{spaxel}
	Obs	Corr	Obs	Corr	Obs	Corr	Obs	Corr	Obs	Corr	Obs	Corr	
NGC2369	1.08	1.21	1.18	1.32	1.19	1.33	0.59	0.66	0.55	0.60	2.30	2.57	1583
NGC3110	0.80	0.84	0.80	0.80	0.85	0.89	0.33	0.34	0.43	0.46	1.46	1.53	2719
NGC3256	1.00	1.04	1.09	1.28	1.20	1.24	0.82	0.84	0.33	0.34	2.90	2.96	5553
ESO320-G030	0.74	0.76	0.69	0.69	0.99	1.02	0.84	0.86	0.35	0.36	2.46	2.53	4011
IRASF12115-4656	0.69	0.73	0.74	0.74	0.73	0.77	0.25	0.26	0.39	0.41	1.20	1.25	3526
NGC5135 (all)	1.31	1.37	1.88	1.88	1.45	1.52	0.84	0.87	0.48	0.50	2.89	3.01	1610
NGC5135 ([SiVI])[2]	1.46	1.53	1.99	1.98	1.54	1.61	0.76	0.79	0.55	0.58	2.82	2.91	898
NGC5135 (no [SiVI])[3]	1.09	1.14	0.68	0.80	1.34	1.40	0.92	0.95	0.44	0.46	2.93	3.06	712
IRASF17138-1017	0.65	0.68	0.58	0.93	0.76	0.79	0.45	0.47	0.22	0.23	1.61	1.68	2327
IC4687	0.540	0.56	0.61	0.61	0.57	0.59	0.29	0.31	0.17	0.18	1.13	1.17	4212
NGC7130 (all)	1.05	1.10	1.11	1.11	1.42	1.47	1.24	1.28	0.26	0.27	4.20	4.33	1857
NGC7130 ([SiVI])[2]	1.79	1.88	1.23	1.22	2.31	2.42	1.42	1.44	0.95	1.06	5.15	5.31	498
NGC7130 (no [SiVI])[3]	0.76	0.79	0.61	1.11	1.09	1.12	0.98	1.01	0.23	0.24	3.12	3.21	1359
IC5179	0.71	0.73	0.84	0.84	0.78	0.80	0.37	0.38	0.32	0.33	1.46	1.49	4490
LIRGs	0.77	0.80	0.79	0.67	0.97	1.01	0.73	0.75	0.29	0.30	2.30	2.38	31888

Table 8: H_2 2.12μm/Brγ line ratios for LIRGs. Values for emission line peaks and integrated measurements

Object	Integrated		Nucleus		HII peak		H_2 peak		[FeII] peak	
	Obs	Corr	Obs	Corr	Obs	Corr	Obs	Corr	Obs	Corr
NGC2369[1,2]	1.10 ± 0.14	1.21 ± 0.78	0.72 ± 0.04	0.77 ± 0.20	0.72 ± 0.04	0.77 ± 0.18	0.73 ± 0.04	0.78 ± 0.19	0.95 ± 0.04	1.04 ± 0.33
NGC3110[2,3]	0.82 ± 0.04	0.90 ± 0.23	0.72 ± 0.04	0.82 ± 0.53	0.62 ± 0.02	0.65 ± 0.13	0.71 ± 0.04	0.82 ± 0.53	0.70 ± 0.04	0.79 ± 1.39
NGC3256	...	...	...	...	...	...	...	...	...	...
ESO320-G030	0.88 ± 0.05	0.93 ± 0.28	5.47 ± 0.46	5.81 ± 1.77	0.46 ± 0.03	0.49 ± 0.11	5.90 ± 0.55	6.26 ± 1.92	4.74 ± 0.36	5.03 ± 1.52
IRASF12115-4656[1,2]	0.84 ± 0.08	0.95 ± 0.84	1.69 ± 0.19	1.92 ± 1.70	1.66 ± 0.19	1.88 ± 1.67	1.69 ± 0.19	1.92 ± 1.70	...	...
NGC5135[2]	1.29 ± 0.07	1.37 ± 0.40	1.70 ± 0.06	1.76 ± 0.41	0.60 ± 0.02	0.62 ± 0.10	1.70 ± 0.06	1.76 ± 0.41	1.62 ± 0.08	1.70 ± 0.44
IRASF17138-1017[2]	0.47 ± 0.02	0.49 ± 0.08	0.49 ± 0.02	0.52 ± 0.15	0.16 ± 0.01	0.17 ± 0.02	0.49 ± 0.02	0.52 ± 0.15	0.26 ± 0.01	0.27 ± 0.03
IC4687[4]	0.38 ± 0.01	0.39 ± 0.04	0.56 ± 0.02	0.59 ± 0.12	0.13 ± 0.01	0.14 ± 0.01	0.68 ± 0.03	0.71 ± 0.16	0.14 ± 0.01	0.15 ± 0.01
NGC7130[1,2,3]	1.41 ± 0.07	1.51 ± 0.94	1.35 ± 0.04	1.42 ± 0.69	1.34 ± 0.04	1.40 ± 0.68	1.37 ± 0.04	1.44 ± 0.72	1.35 ± 0.04	1.42 ± 0.69
IC5179[1,2,3]	0.66 ± 0.03	0.68 ± 0.17	0.49 ± 0.02	0.51 ± 0.06	0.47 ± 0.02	0.49 ± 0.06	0.49 ± 0.02	0.50 ± 0.06	0.47 ± 0.02	0.48 ± 0.06

3. Results

3.3. Understanding the near-IR emission line diagnostic diagram for star-forming galaxies and AGN

3.3.1. LIRGs in the [FeII]1.64μm/Brγ – H$_2$2.12μm/Brγ plane

● Range from pure-star-forming to AGN
(Threshold is discussed in later sections 3.3.2-3.3.4)

● No region showing log([FeII]/Brγ)>1.0 & log(H$_2$/Brγ)>0.8, i.e. LINERS defined in Riffel+2013a

→ Surprising results

● All LIRGs but two are classified as SF with mid-IR and X-ray

● Star-formation and LINERs with optical emission lines

Study with 3 prototypes (SF, AGN, Composite LIRG)

5 type region

1. Bright compact Brγ emitting regions
2. Bright compact [FeII] emitting regions
3. Bright compact [SiVI] regions
4. Diffuse extended [SiVI] emitting regions
5. Diffuse extended non-[SiVI] emitting regions

Fig. 1
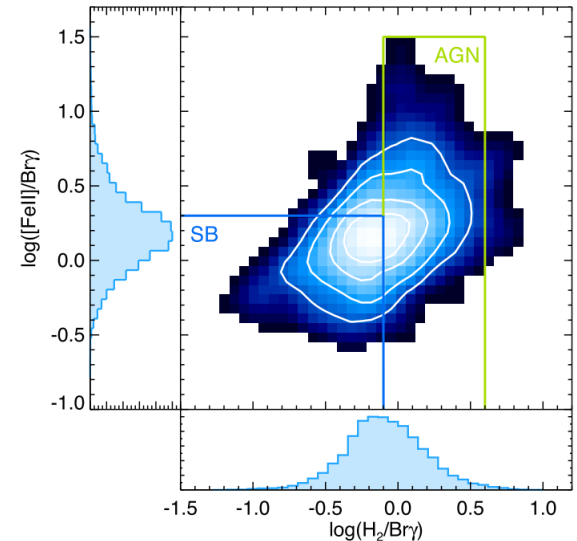
Identify these emitting regions in the prototypes and constrain the line ratio produced by different ionization source

3. Results

3.3.2. IC 4687: prototype of LIRG dominated by star formation

Brγ: Several circumnuclear star-forming clump and weak nucleus

H_2: Very diffuse and distributed over the entire circumnuclear region

[FeII]: Follow that of the Brγ clumpy distribution

In the [FeII]1.64μm/Brγ − $H_2$2.12μm/Brγ

- The mode is outside of the previously identified region for SFGs (Riffel+2013a)
- Long tail towards low values
- Bright Brγ regions identify young SF region with both ratio < 1
- Nuclear region is identified with evolved, supernova dominated SF region and well separated with about x6 values of ratios
- Diffuse region
  - SF < [FeII]/Brγ < SNe
  - H_2/Brγ ~ SNe

Fig. 2
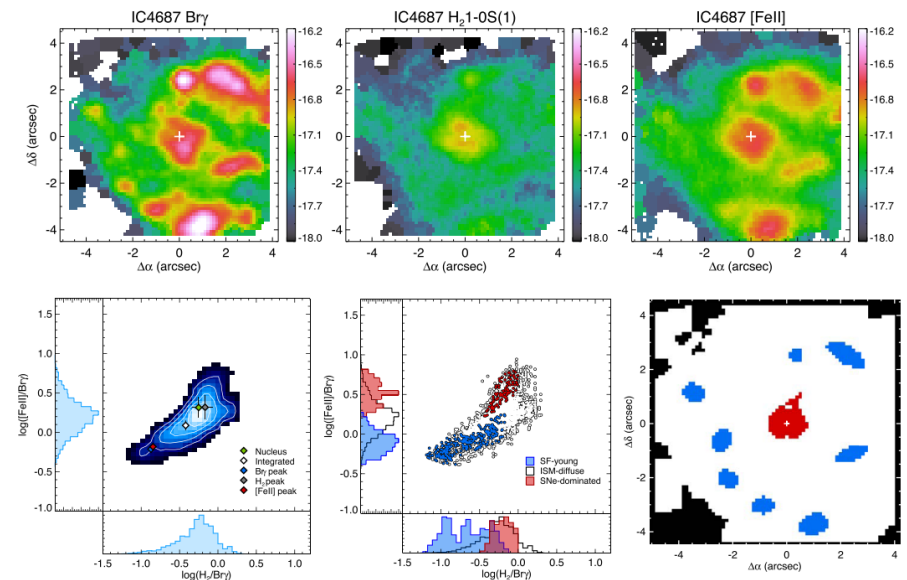
3. Results

3.3.3. NGC 7130: prototype of a LIRG dominated by a Seyfert 2 nucleus

Nucleus: Known Seyfert 2-type AGN (Levenson+2005, Alonso-Herrero+2012)
and the presence of [SiVI]1.96μm

Previous optical: Smooth transition from AGN in the center to SF in the external region

Previous UV, mid-IR: Presence of young star clusters and PAH emission (star-formation)

In the [FeII]1.64μm/Brγ – $H_2$2.12μm/Brγ

- Compact [SiVI] emitting region (AGN):
  Exclusively the highest (>5) [FeII]/Brγ values

- Brγ circumnuclear region (Young SF clump):
  Similar to SF region of IC 4687

- Weak [SiVI] emitting region (AGN-diffuse):
  Highest end of the H_2/Brγ
  and intermediate [FeII]/Brγ values

- Diffuse non-[SiVI]:
  Wide range of H_2/Brγ values
  and slightly higher [FeII]/Brγ than SF clump

Fig. 3 (Contour:[SiVI] emission)
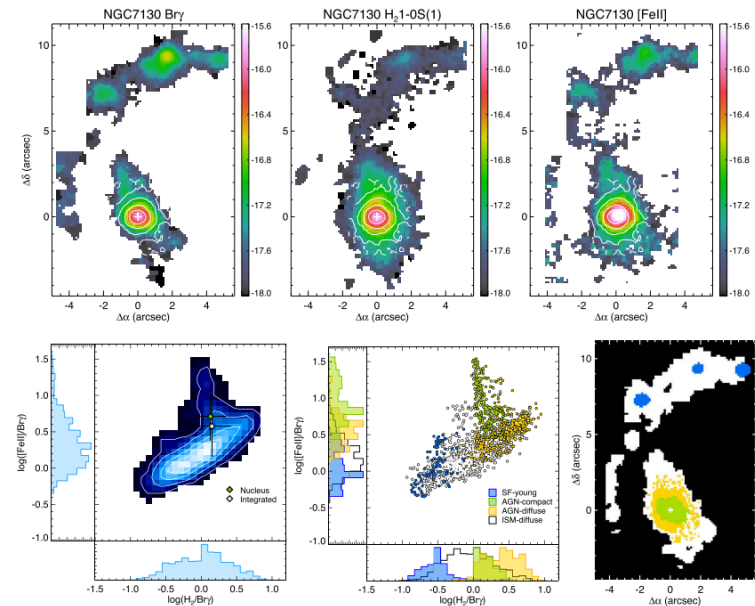
3. Results

3.3.4. NGC 5135: prototype of composite LIRG

Consists of Seyfert2 nucleus, young massive stars and supernovae

All the region are within a radius of 600 pc → Unresolved composite LIRG in high-z

In the [FeII]1.64µm/Brγ – $H_2$2.12µm/Brγ

- **Young star forming clumps**:
  Similar to that of young SF in IC4687 and NGC7130

- **SNe-dominated star-forming clump**:
  Very high [FeII]/Brγ ratios (~3 - 16) consistent with SNe remnants

- **AGN-dominated nuclear region**:
  H_2/Brγ ~ SNe-dominated clump
  [FeII]/Brγ is ~3.5 lower than SNe

- **AGN-diffuse region**:
  Occupies mostly the region of AGN, overlapping with SNe, disentangled from SF clumps

- Diffuse ISM: SF < [FeII]/Brγ < AGN, H_2/Brγ covering the range of all the sources

Fig. 4
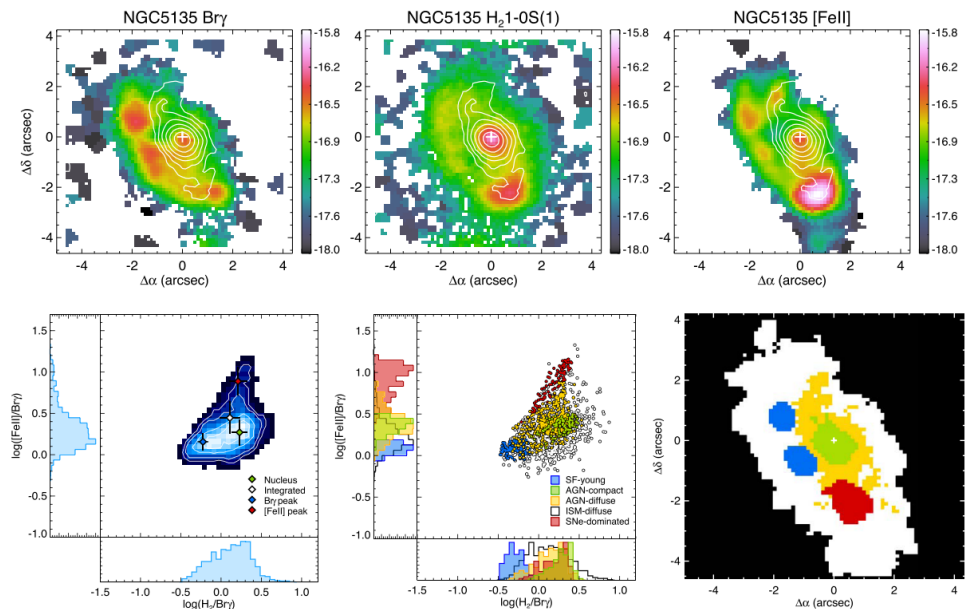
3. Results

3.3.4. Cont'd

Interpretations for Compact regions

- Aged (~8-40 Myr) SNe-dominated vs Young (<6 Myr) star-forming clumps
    1. Enhancement of iron abundance and emission due to SNe (increased [FeII])
    2. Larger relative amount of ionizing photons in young clumps (increased Brγ)
    3. Larger relative importance of shocks and X-ray emission associated with SNe (increased H_2)
- AGN-dominated vs Young star-forming clumps
    - Larger amount of X-ray with respect to UV-ionizing radiation in the AGN
      → Excess of X-ray penetrate more deeply in surrounding medium, producing a larger partially ionized region (enhanced [FeII] and H_2)
    - X-ray studies in NGC 5135 (Colina+2012): Hard X-ray at nucleus and SNe clump
      Soft X-ray covering the circumnuclear region
    - K-band H_2 emission line ratios of the nucleus and SNe region consistent with predicted thermal raios, young SF region depart from thermal (Bedregal+2009)

Interpretation for Diffuse regions

- Consequence of the leaking of different radiation field
    - H_2/Brγ appears to be associated with the leaking of X-rays from AGN and SNe clump
    - [FeII]/Brγ appears to be associated with UV-radiation
    - Not consider the effect of shock enhancing the [FeII] emission as in NGC4151 (Storchi-Bergmann+2009)

4. Discussion

4.1. LIRGs and Seyferts. Defining new near-IR line ratio limits and relations to discriminate activity in galaxies

New limits and relation as a function of location within galaxy → 2D distribution vs Integrated light → High-redshift studies

For compact, high-surface brightness regions

- SF-young
  - $\log([FeII]/Br\gamma) = 0.238 + 0.476 \times \log(H_2/Br\gamma)$
  - $-1.2 < \log(H_2/Br\gamma) < -0.1$
  - $-0.4 < \log([FeII]/Br\gamma) < +0.4$

- SNe-dominated
  - $\log([FeII]/Br\gamma) = 0705 + 1.000 \times \log(H_2/Br\gamma)$
  - $-0.4 < \log(H_2/Br\gamma) < +0.4$
  - $+0.2 < \log([FeII]/Br\gamma) < +1.2$

- AGN-compact
  - $\log([FeII]/Br\gamma) = 1.009 - 1.312 \times \log(H_2/Br\gamma)$
  - $-0.3 < \log(H_2/Br\gamma) < +0.9$ (?)
  - $-0.3 < \log([FeII]/Br\gamma) < 1.5$ (?)

Fig. 5 (Part): For 3 prototypes
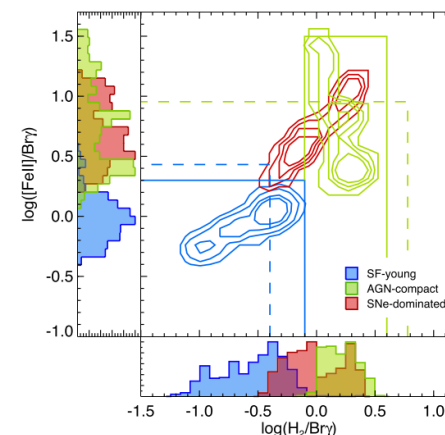
Fig. 6 (Part): For all LIRGs
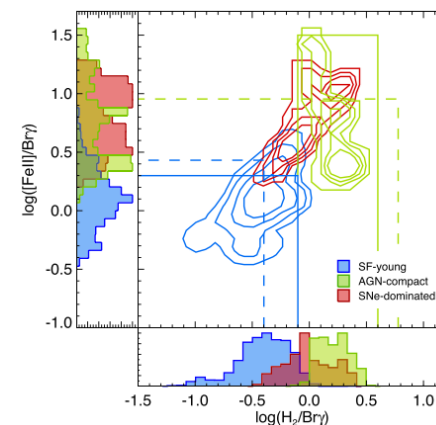
4. Discussion

4.1. Cont'd

For the diffuse medium

Fig. 5 (Part): For 3 prototypes

- AGN-diffuse
  - Similar to AGN-compact but not extreme in [FeII]/Brγ
  - Linear relation $\log([FeII]/Br\gamma) = 0705 + 1.000 \times \log(H_2/Br\gamma)$
  - -- Slope is close to SF-clump but depart from Riffel+2013a(0.749)
  - → Because of the subtraction of the stellar absorption and continuum in Riffel's LINER galaxies with weak emission lines
  - → Overestimation of ratio with underestimation of hydrogen lines

- Diffuse ISM
  - Cover wide range of values
  - → Mixture of that of individual heating sources (Young stars, SNe, AGN, shocks, etc.) weighted by their relative flux contribution and spatial distribution
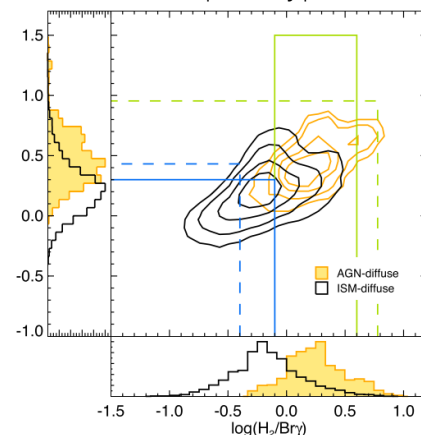
Fig. 6 (Part): For all LIRGs

4. Discussion

4.2. Excitation mechanisms: bright, compact line-emitting regions

Consider only the peak regions of emission lines

- Most of them are located close to the mode or lower ratio area

- Agree with the nucleus and off-nuclear regions of solar metallicity galaxies (M82, NGC4303)
  ↔ Well above the values for low-metallicity galaxies (Mrk59, NGC1569W)

- A small fraction of regions are in SNe-dominated or AGN-dominated

- Different behavior of two galaxies with Seyfert2 nucleus (NGC7130 vs NGC5135)

  - NGC5135 has significantly lower [FeII]/Brγ
    → Mixture of AGN and young stars with different relative contributions,
      and/or aging effect of nuclear star clusters

- ESO320-G030
  as outlier with high H_2/Brγ
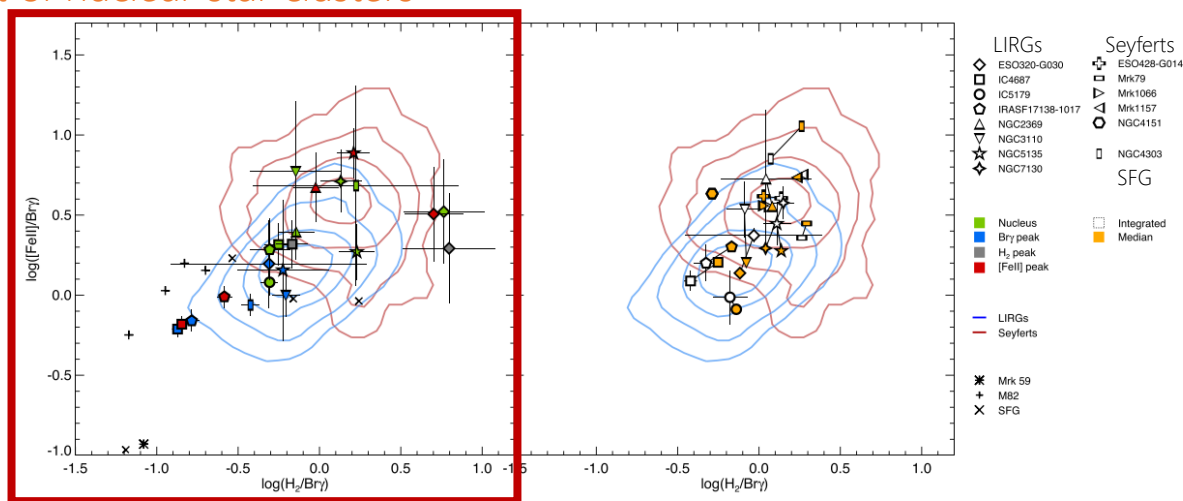
4. Discussion

4.3. Spatially resolved versus integrated line ratios.
Implication for the classification of high-z star-forming galaxies

Integrated value (flux-weighted measurements) → Dominated by the brightest regions

Comparison between flux-weighted(integrated) and median for LIRGs

- Only one (IC5179) shows the difference less than 0.1 dex
- Two (IC4687&IRASF17138-1017) show integrated value lower than median (x0.5-0.6)
- The rest show integrated [FeII]/Brγ value ~1.5-2.2 times higher than median
  → Moving towards the locus of AGN

Only in LIRG? General behavior of galaxies (Martins+2013 for star-forming galaxies)?

Need further explorations.